Electronic Supplementary Information

Interaction of aryl tetrazolones with anions: Proton transfer Vs hydrogen bonding

Erika Nord, Hanyang Zhou and Sundeep Rayat*

Department of Chemistry, Ball State University, Cooper Physical Science Building, Muncie, IN 47304 - 0445, United States.

srayat@bsu.edu

Experimental Procedures

All chemicals used in the syntheses were purchased from Aldrich or Fisher Scientific. Tetrabutyl ammonium salts (TBAA, TBAB, $TBANO_3$, TBACl, and $TBAHSO_4$) used for anion-binding studies were purchased from Aldrich. Tetrapropyl thiocyanate (TPANCS) salt was prepared from KNCS and tetrapropyl tetrafluoroborate.[1] All chemicals were used without additional purification. The salts were stored in a desiccator (TBAB, $TBAHSO_4$, $TBANO_3$) or glove box (TBAA and TBACl), as they were extremely hygroscopic. ^{1}H NMR spectra were obtained on a JEOL 400MHz NMR spectrometer in 99.9 atom % DMSO-d_6. The NMR spectra were processed using MestReNova Software. UV spectra were obtained on a UV-VIS Spectrophotometer 2600. UV titrations with anions were performed in a 1mm quartz cuvette and the sample holder was regulated at a consistent temperature of 25 ^{o}C, while the UV spectra with triethylamine were obtained using 1cm quartz cuvette. All UV solutions were prepared in HPLC grade acetonitrile. Gas-tight syringes were used to prepare all NMR and UV samples. UV titrations were conducted at high concentration of the host (**1a**,**b**) to ensure the detection of the host-guest complex [**1a**,**b**----A^-] in case of a low association constant K_a, and low molar absorptivity of the host-guest complex. Low resolution mass spectra (LRMS) were obtained on a

mass spectrometer equipped with an electrospray ion source operated in the negative ion mode and connected to a linear ion trap mass analyzer.

Computational methods

All calculations were performed using the Gaussian 09 package of programs.[2] Optimized geometries of all stationary points on the potential energy surface were obtained using the Density Functional Theory (M062X) with the employment of 6-311+G* basis set. The geometries were fully optimized without any symmetry constraints in the presence of polarized continuum model to approximate the acetonitrile environment. Optimizations were followed with vibrational analysis to ensure an imaginary frequency of zero for the ground states. The binding enthalpies with corrected basis set superposition error were calculated by counterpoise method.[3] The molecular electrostatic potentials (MESP) plots and surface minima (Vs,min) as well as surface maxima (Vs,max) were calculated and visualized using GaussView.[4]

Figure S1. Structure of tetrazolonide anion **1a'** and **1b'** optimized at M06-2X/6-311+G*/PCM=MeCN.

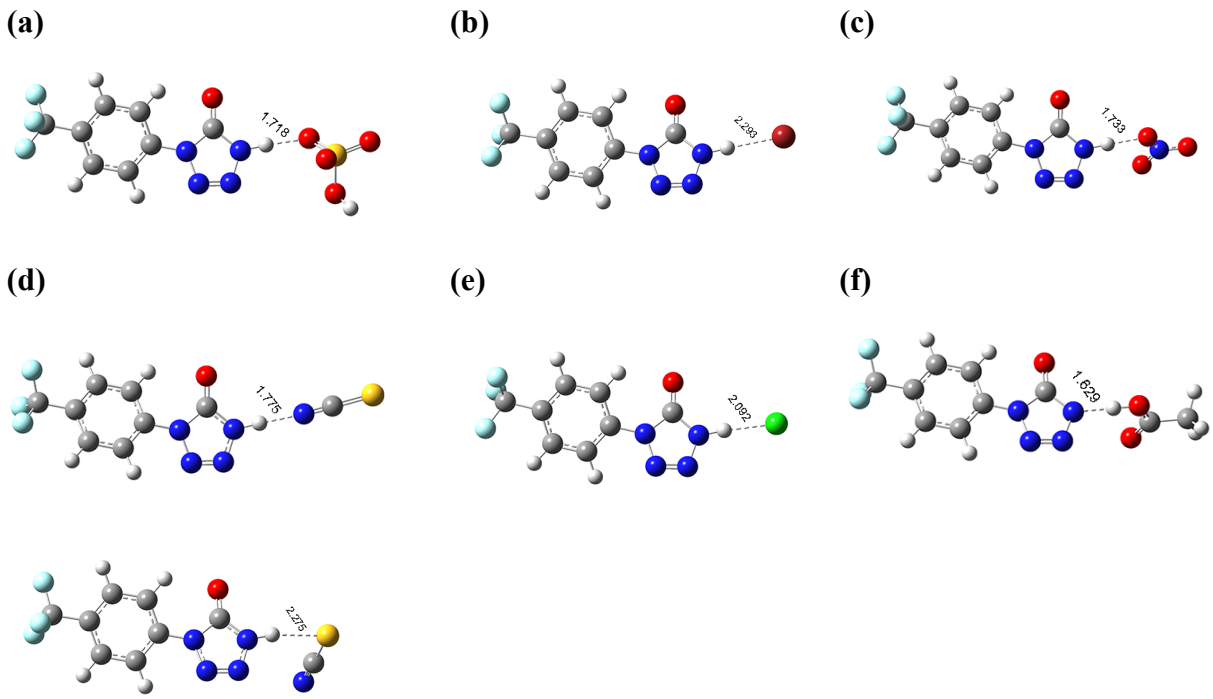

Figure S2. Complexes of **1b** with (a) HSO_4^-, (b) Br^-, (c) NO_3^-, (a) NCS^-, and (e) Cl^- optimized at M06-2X/6-311+G*/PCM=MeCN, and (f) proton transfer during optimization of **1b** with AcO^-. Distances are in Å.

Synthesis of tetrazolones

Trimethylsilyl azide ($TMSN_3$) (1.5 mmol) was added to the corresponding aryl isocyanate (1.0 mmol) in a round bottom flask. The resulting mixture was refluxed at 100 °C for 24 hours. TLC was used to monitor the reaction. When complete, the reaction mixture was cooled to room temperature and the excess $TMSN_3$ was removed under reduced pressure. The crude solid was purified by recrystallization with ethanol.

Synthesis of p-nitrophenyltetrazolone 1a[5]

$TMSN_3$ (0.30 mL, 2.28 mmol) was added to *p*-nitrophenyl isocyanate (0.250 g, 1.52 mmol) in a round bottom flask. The crude solid was recrystallized with ethanol. The desired compound **1a** was a pale-yellow solid (0.23 g, 72% yield). R_f = 0.11 (7:3 hexane/ethyl acetate); ^{1}H NMR (400 MHz, DMSO-d_6): δ 8.19 (d, *J* = 9.2 Hz, 2H), 8.43 (d, *J* = 9.2 Hz, 2H), 14.99 (s, 1H).

Synthesis of p-trifluoromethylphenyltetrazolone 1b[6]

$TMSN_3$ (0.53 mL, 4.01 mmol) was added to *p*-trifluoromethylphenyl isocyanate (0.500 g, 2.67 mmol) in a round bottom flask. The crude solid was purified with column chromatography using a gradient elution of 8:2 hexane and ethyl acetate. The desired compound **1b** was a white solid (0.26 g, 43% yield). R_f = 0.13 (8:2 hexane/ethyl acetate); ^{1}H NMR (400 MHz, DMSO-d_6): δ 7.94 (d, *J* = 8.6 Hz, 2H), 8.13 (d, *J* = 8.5 Hz, 2H), 14.91 (s, 1H). LRMS(ESI): m/z 229 ($M\text{-}H^+$).

Determination of molar absorptivities of 1a,b

3 mM stock solutions of **1a,b** were prepared in acetonitrile. Four 1 mL working solutions with concentrations of 3, 2.25, 1.5, and 0.75 mM were obtained using the stock. UV spectra of these samples were recorded to determine molar absorptivities using Beer-Lambert Law (Figure S3 and Table S1).

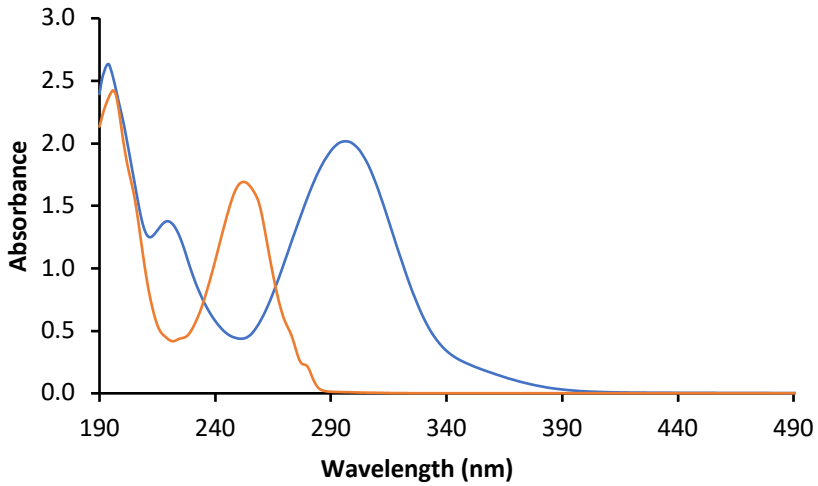

Figure S3. UV absorption spectra of **1a**,**b** in acetonitrile (0.0015 M). **1a**-blue; **1b**-red.

Table S1. Molar absorptivity values for UV bands of 1a,b in acetonitrile.

	λ_1 (ε_1)	λ_2 (ε_2)	λ_3 (ε_3)
1a	297 (10341)	220 (6899)	193 (9365)
1b	252 (7796)	196 (7644)	

Anion-binding studies

UV titrations of 1a,b with HSO_4^-, Br^-, NO_3^-, NCS^-, Cl^-, and AcO^-

Stock solutions of tetrazolones **1a,b** (host) and tetrabutylammonium (for HSO_4^-, Br^-, NO_3^-, Cl^-, and AcO^-) or tetrapropylammonium (for NCS^-) salts of the anions (guests) were prepared in acetonitrile in volumetric flasks (Table S2).

Table S2. Concentration of each stock solution of the anion for UV titrations.

Anion	**1a**[a] (M)	**1b**[a](M)
HSO_4^-	0.350	0.189
Br^-	0.109	0.106
NO_3^-	0.244	0.244
NCS^-	0.275	
Cl^-	0.0165	0.0188
AcO^-	0.8	0.9

[a]Stock solutions of **1a,b** were 3mM in acetonitrile, except for titration with Cl^- where the concentrations for **1a** and **1b** were 0.5 and 0.6 mM, respectively.

For each UV titration, twelve samples were prepared by measuring the volumes specified in Table S3 with a gas tight syringe. Each sample was mixed by gentle shaking for five minutes before being transferred to a 1 mm cuvette to record a UV spectrum.

Table S3. Amount of stock solutions of 1a,b and the anions used for the UV titrations.

Sample	1a,b (mL)	Anion (mL)	MeCN (mL)
1	0.500	0	0.500
2	0	0.300	0.700
3	0.500	0.500	0
4	0.500	0.350	0.150
5	0.500	0.270	0.230
6	0.500	0.190	0.310
7	0.500	0.120	0.380
8	0.500	0.080	0.420
9	0.500	0.050	0.450
10	0.500	0.030	0.470
11	0	0.100	0.900
12	0.500	0	0.500

The difference spectrum was a plot of the A_{HG} vs. wavelength (nm). A_{HG} is the host-guest (HG) complex absorbance and was obtained from the equation below, where A_{mix} is the observed absorbance of the mixture, A_{host} is the observed absorbance of the host, and A_{guest} is the absorbance of the guest.

$$A_{HG} = A_{mix} - A_{host} - A_{guest}$$

A_{guest} was obtained as follows:

$$A_{guest} = \varepsilon_{guest} \text{ x } [G_o]_{mix}$$

Where, ε_{guest} is the molar absorptivity of the guest, and $[G_o]_{mix}$ is the concentration of guest in the mixture.

Determining association constants

Association constants, K_a, were calculated by utilizing the following equation for curve fitting.[7]

$$A_{HG} = \varepsilon_{HG} \frac{([G_o] + [H_o] + \frac{1}{K_a}) - \sqrt{([G_o] + [H_o] + \frac{1}{K_a})^2 - 4[G_o][H_o]}}{2}$$

In this equation, $[G_o]$ is the concentration of the guest (anion) in the mixture and $[H_o]$ is the concentration of the host (**1a**,**b**) in the mixture. A_{HG} is the HG complex absorbance and ε_{HG} is the molar absorptivity of the complex.

NMR titration of 1a,b with HSO_4^-, Br^-, NO_3^-, Cl^- and AcO^-

For NMR titrations in DMSO-d_6, 25 mM stock solutions of **1a,b** and stock solutions of $TBAHSO_4$, TBABr, $TBANO_3$, TBACl and TBAA (See Table S4 for concentrations) were prepared. These stocks were used to prepare 0.6 mL samples for NMR analyses, where the concentration of tetrazolone was 10 mM, and different equivalents of the anions were added as indicated in (Figures S15 - S24). The samples were mixed by gentle shaking for five minutes before being transferred to an NMR tube to obtain the spectra.

*Note: Data for NMR titration of **1a,b** with HSO_4^-, Br^-, and NO_3^- is not shown as those didn't produce any changes in the spectrum during the titration.*

Table S4. Concentration of each stock solution of the anion for NMR titrations.

Anion	M
HSO_4^-	0.050
Br^-	0.050
NO_3^-	0.050
Cl^-	0.083
AcO^-	0.033

(a) (b)

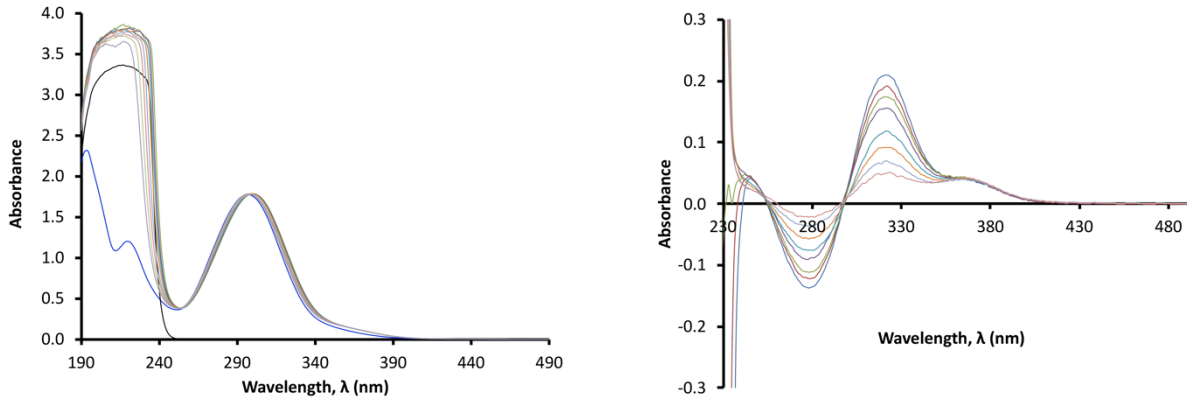

Figure S4. UV titration of 1.5 mM solution of **1a** (a) with increasing amounts of Br^- in acetonitrile (the spectrum of the anion is also shown in black) and (b) the corresponding difference spectrum displaying the increased absorption at 321nm. The concentration of Br^- ranged between 3 – 54 mM).

(a) (b)

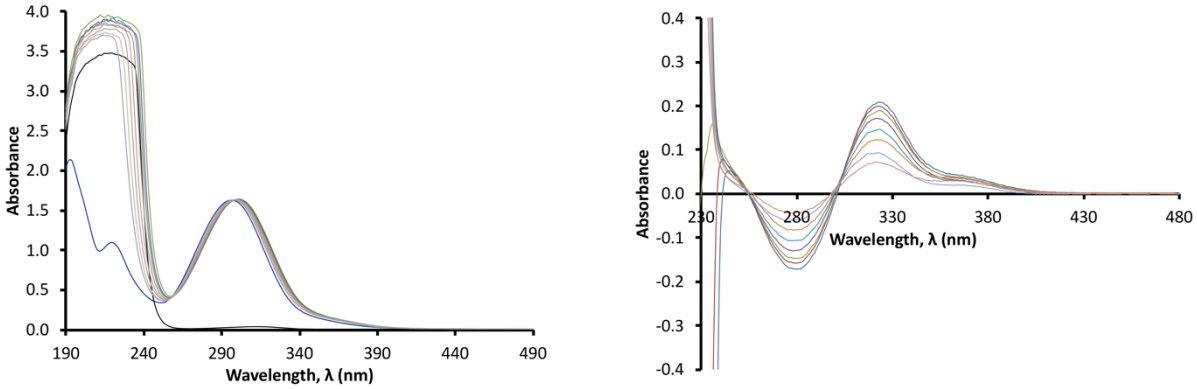

Figure S5. UV titration of 1.5 mM solution of **1a** (a) with increasing amounts of NO_3^- in acetonitrile (the spectrum of the anion is also shown in black) and (b) the corresponding difference spectrum displaying the increased absorption at 321nm. The concentration of NO_3^- ranged between 7 – 122 mM).

(a) (b)

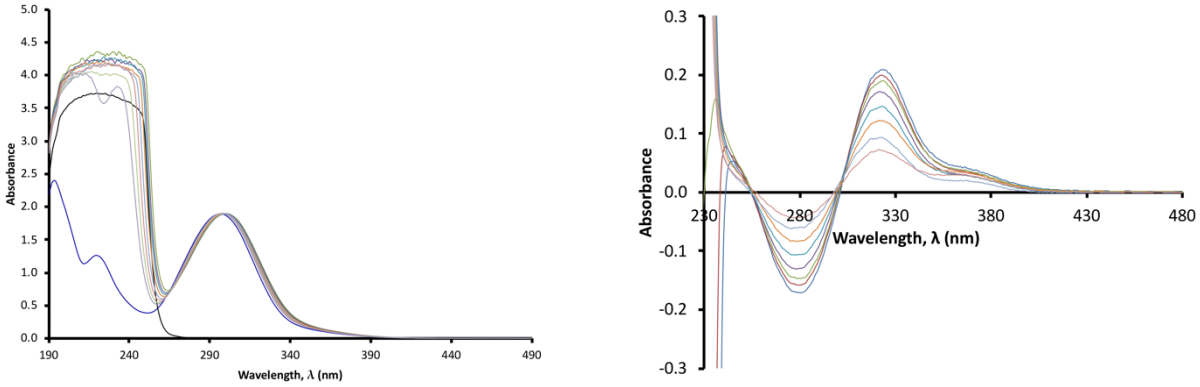

Figure S6. UV titration of 1.5 mM solution of **1a** (a) with increasing amounts of NCS^- in acetonitrile (the spectrum of the anion is also shown in black) and (b) the corresponding difference spectrum displaying the increased absorption at 321nm. The concentration of NCS^- ranged between 8 – 137 mM).

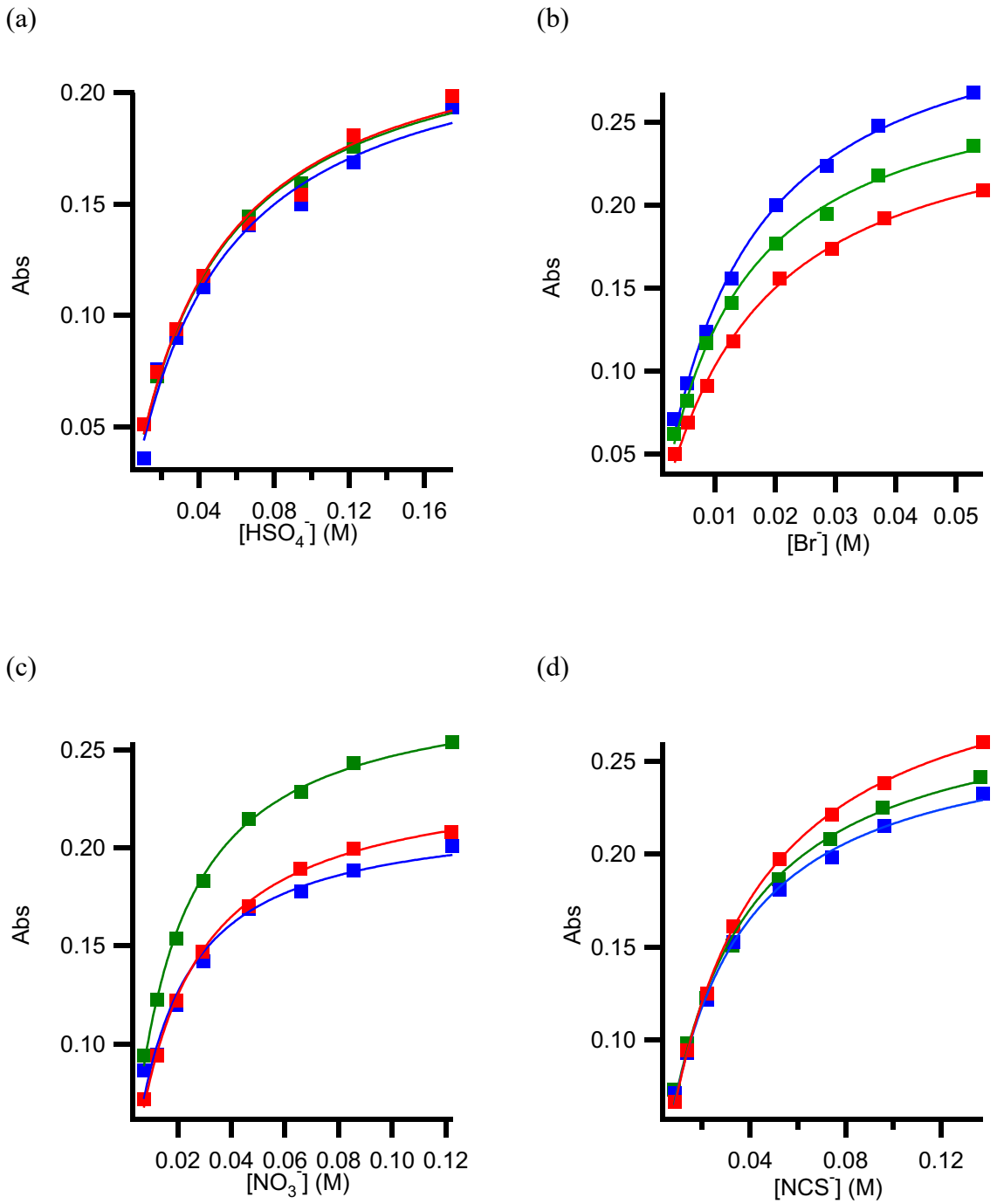

Figure S7. Binding isotherms for each UV titration of **1a** with (a) HSO_4^-, (b) Br^-, (c) NO_3^- and (d) NCS^-

(a) (b)

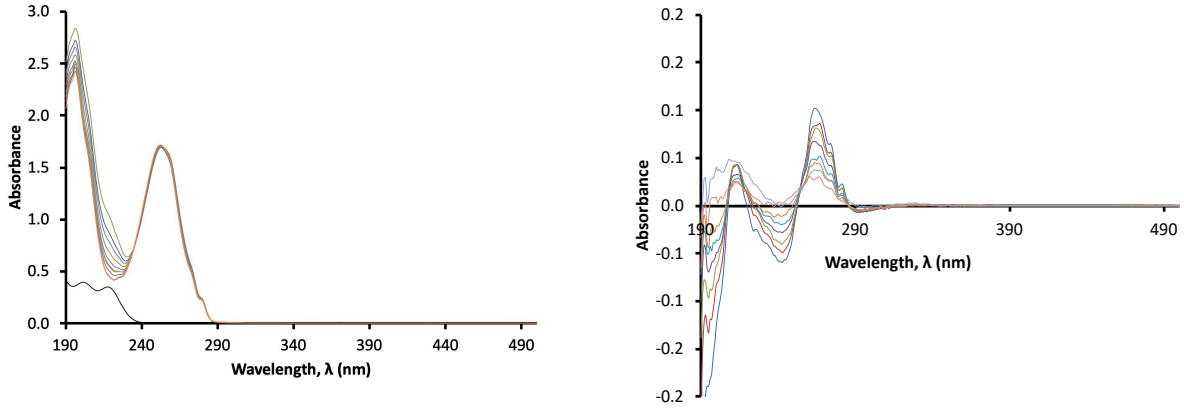

Figure S8. UV titration of 1.5 mM solution of **1b** (a) with increasing amounts of HSO_4^- in acetonitrile (the spectrum of the anion is also shown in black) and (b) the corresponding difference spectrum displaying the increased absorption at 263 nm. The concentration of HSO_4^- ranged between 6 – 94 mM.

(a) (b)

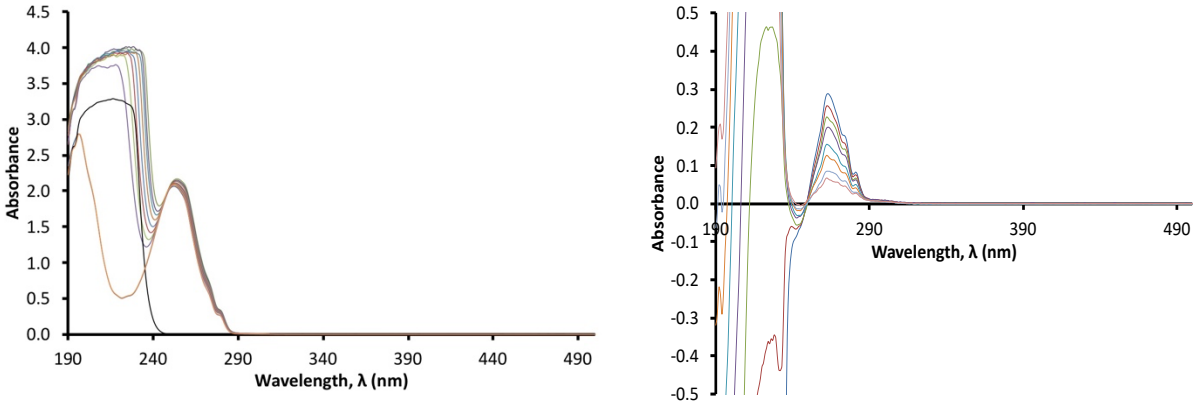

Figure S9. UV titration of 1.5 mM solution of **1b** (a) with increasing amounts of Br^- in acetonitrile (the spectrum of the anion is also shown in black) and (b) the corresponding difference spectrum displaying the increased absorption at 263 nm. The concentration of HSO_4^- ranged between 3 – 53 mM.

(a) (b)

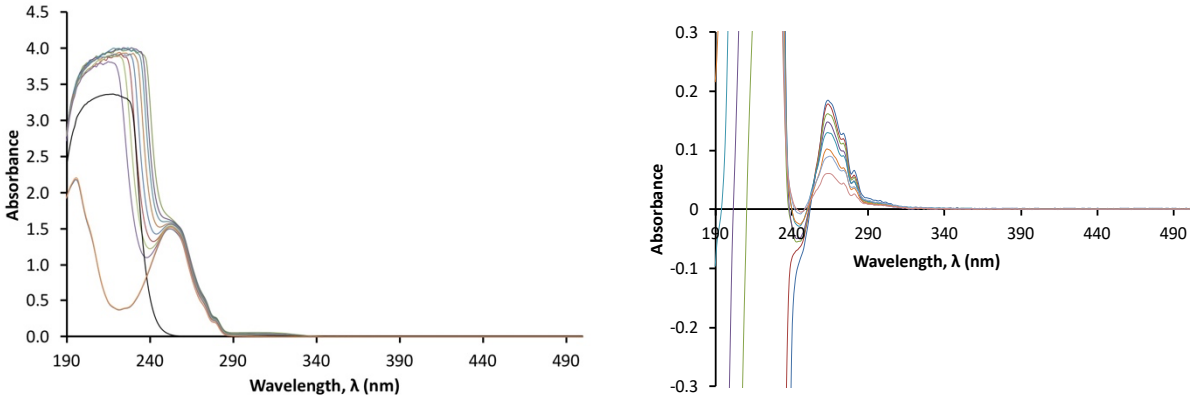

Figure S10. UV titration of 1.5 mM solution of **1b** (a) with increasing amounts of NO_3^- in acetonitrile (the spectrum of the anion is also shown in black) and (b) the corresponding difference spectrum displaying the increased absorption at 263 nm. The concentration of HSO_4^- ranged between 7 – 122 mM.

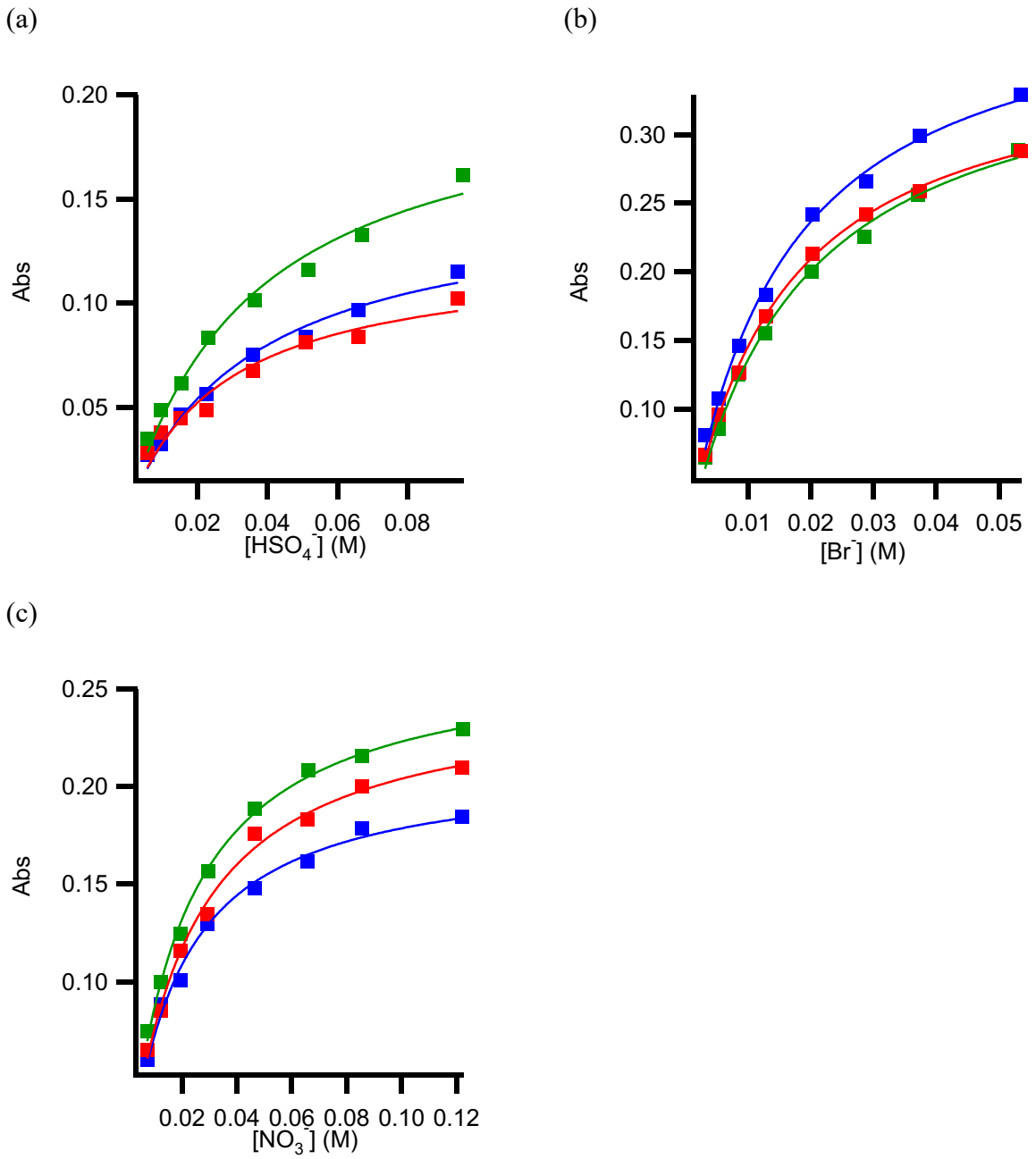

Figure S11. Binding isotherms for each UV titration of **1b** with (a) HSO_4^-, (b) Br^-, and (c) NO_3^-.

(a) (b)

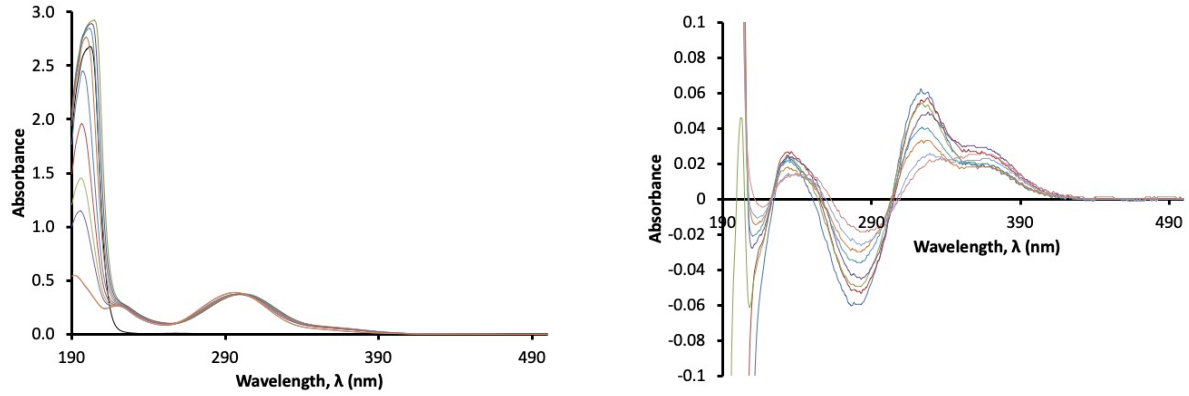

Figure S12. UV titration of 0.25 mM solution of **1a** (a) with increasing amounts of Cl^- in acetonitrile (the spectrum of the anion is also shown in black) and (b) the corresponding difference spectrum displaying the increased absorption at 321 nm. The concentration of Cl^- ranged between 0.4 – 8 mM.

(a) (b

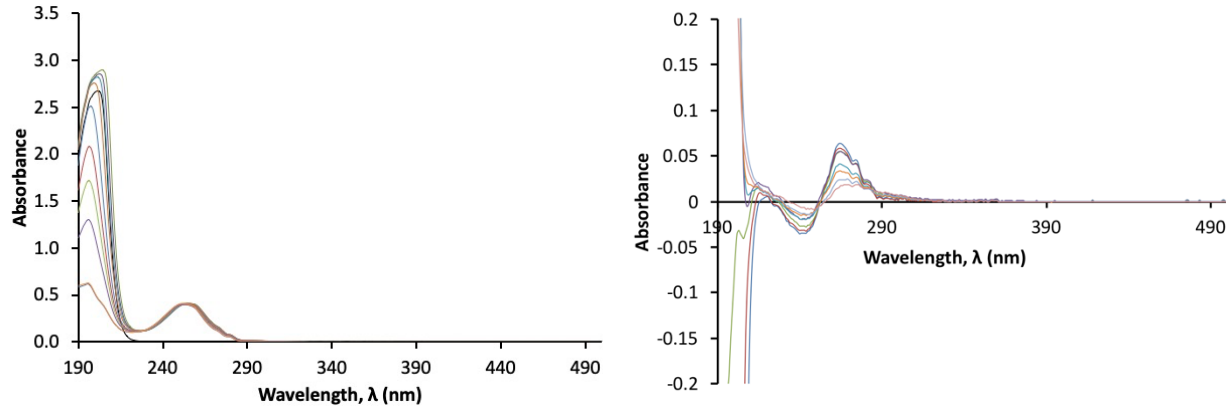

Figure S13. UV titration of 0.3 mM solution of **1b** (a) with increasing amounts of Cl^- in acetonitrile (the spectrum of the anion is also shown in black) and (b) the corresponding difference spectrum displaying the increased absorption at 263 nm. The concentration of Cl^- ranged between 0.5 – 9 mM.

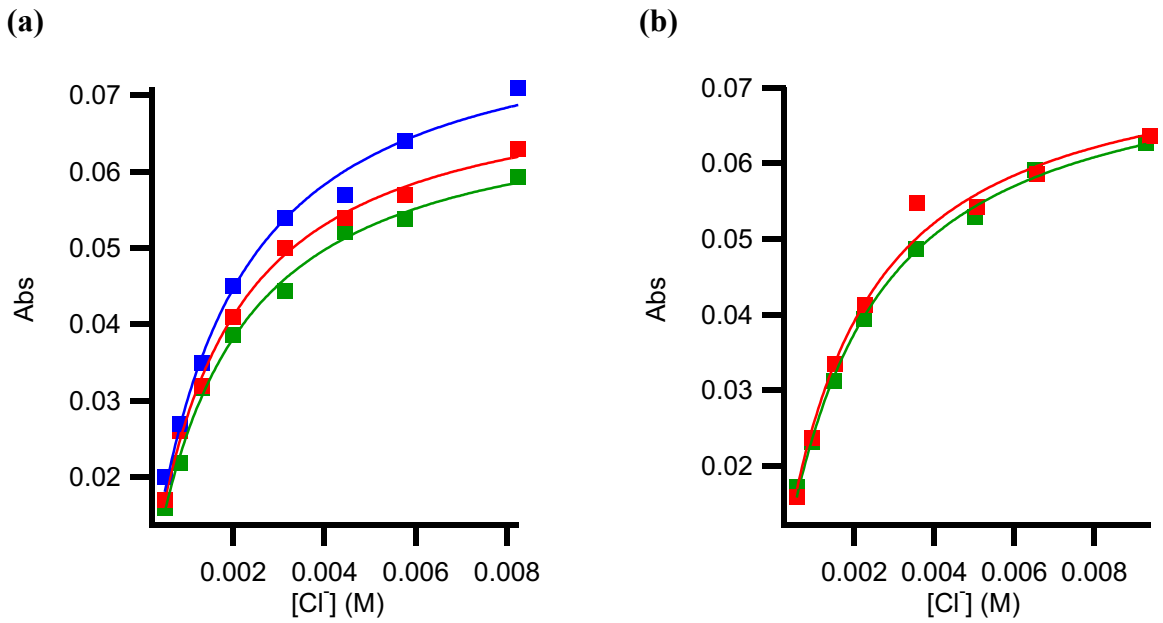

Figure S14. Binding isotherms for each UV titration of **1a** and **1b** with Cl^-.

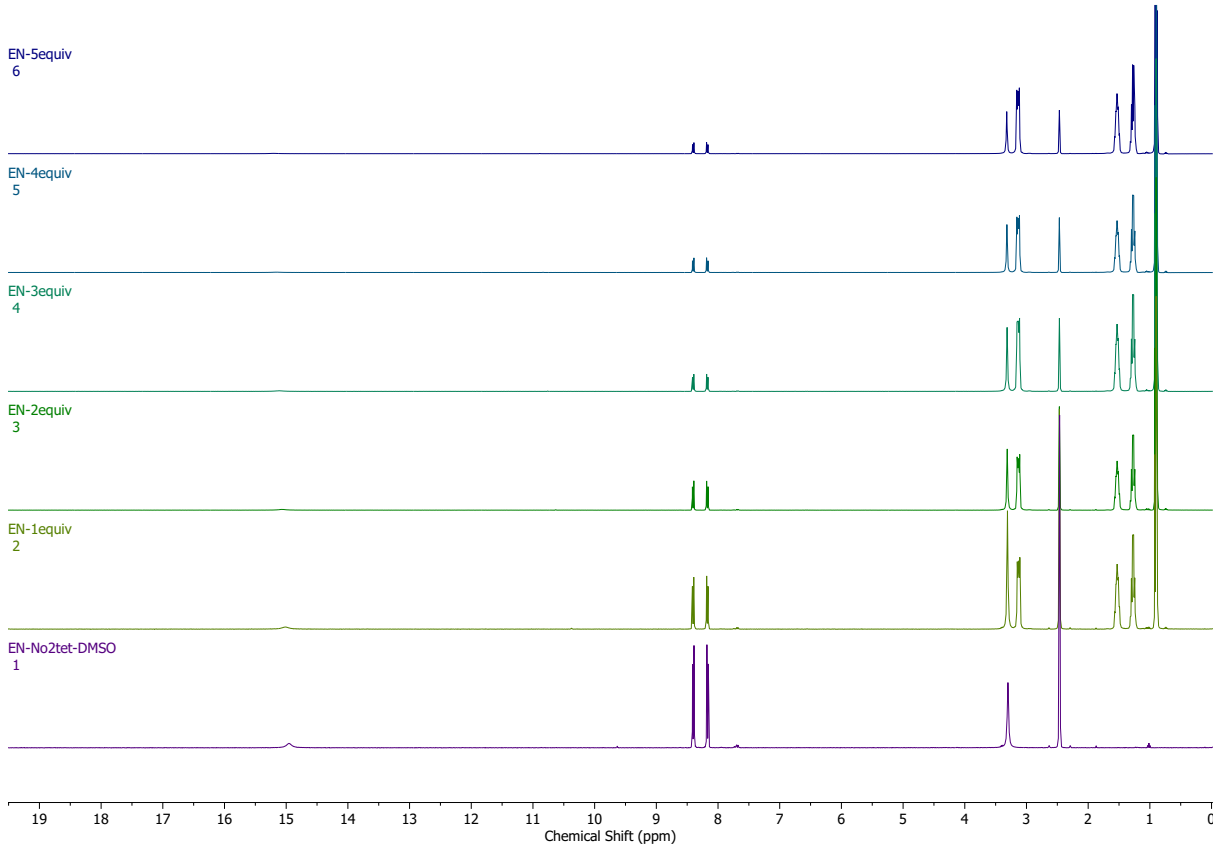

Figure S15. Full NMR spectra of **1a** in DMSO-d_6 with increasing amounts of tetra butyl ammonium chloride (TBACl) from bottom to top.

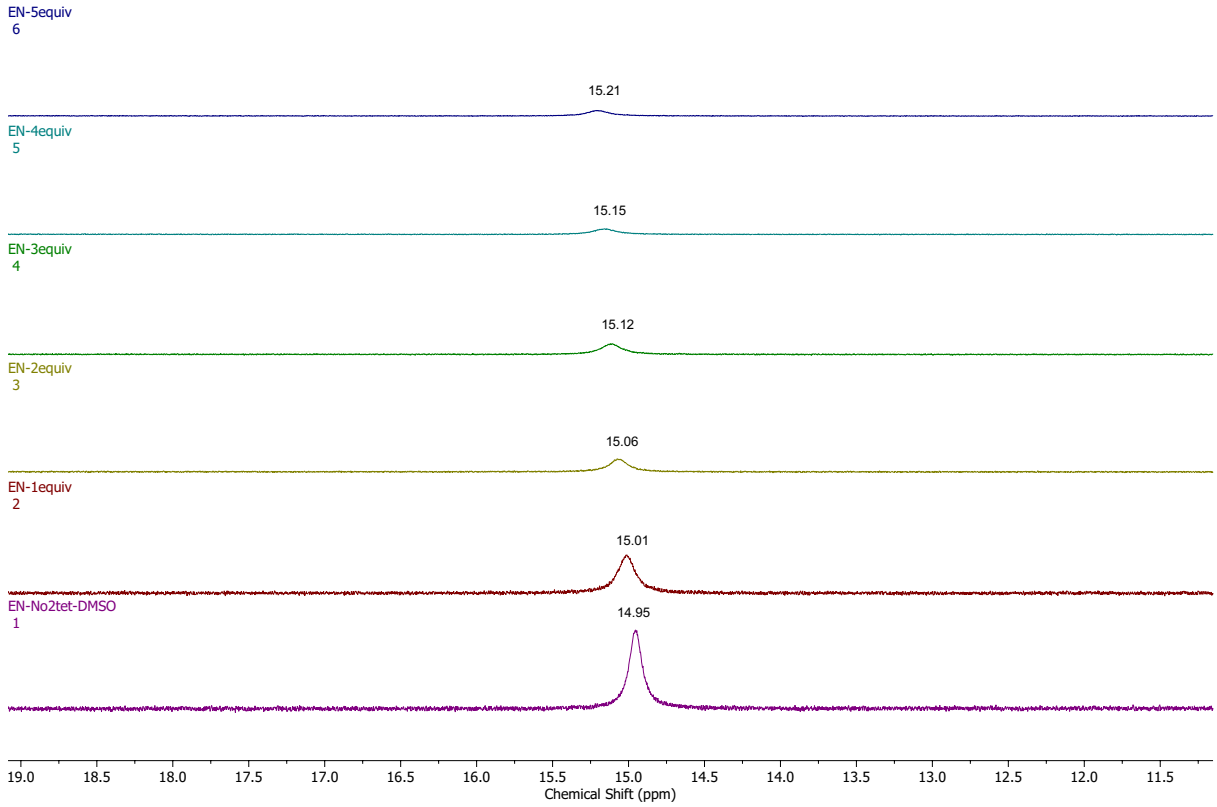

Figure S16. Partial NMR spectra showing changes in the chemical shift of NH proton during the titration of **1a** with increasing amounts of tetra butyl ammonium chloride (TBACl) in DMSO-d_6 from bottom to top.

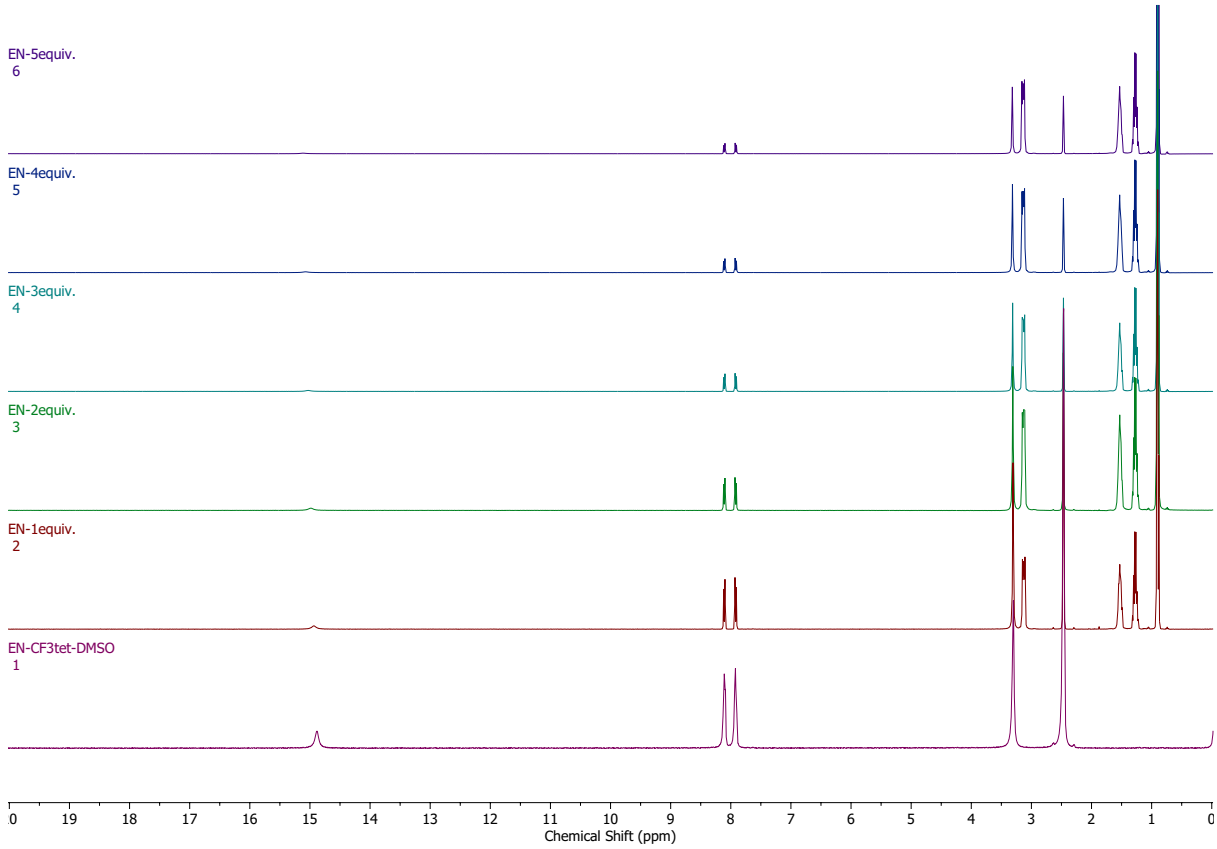

Figure S17. Full NMR spectra of **1b** in DMSO-d_6 with increasing amounts of tetra butyl ammonium chloride (TBACl) from bottom to top.

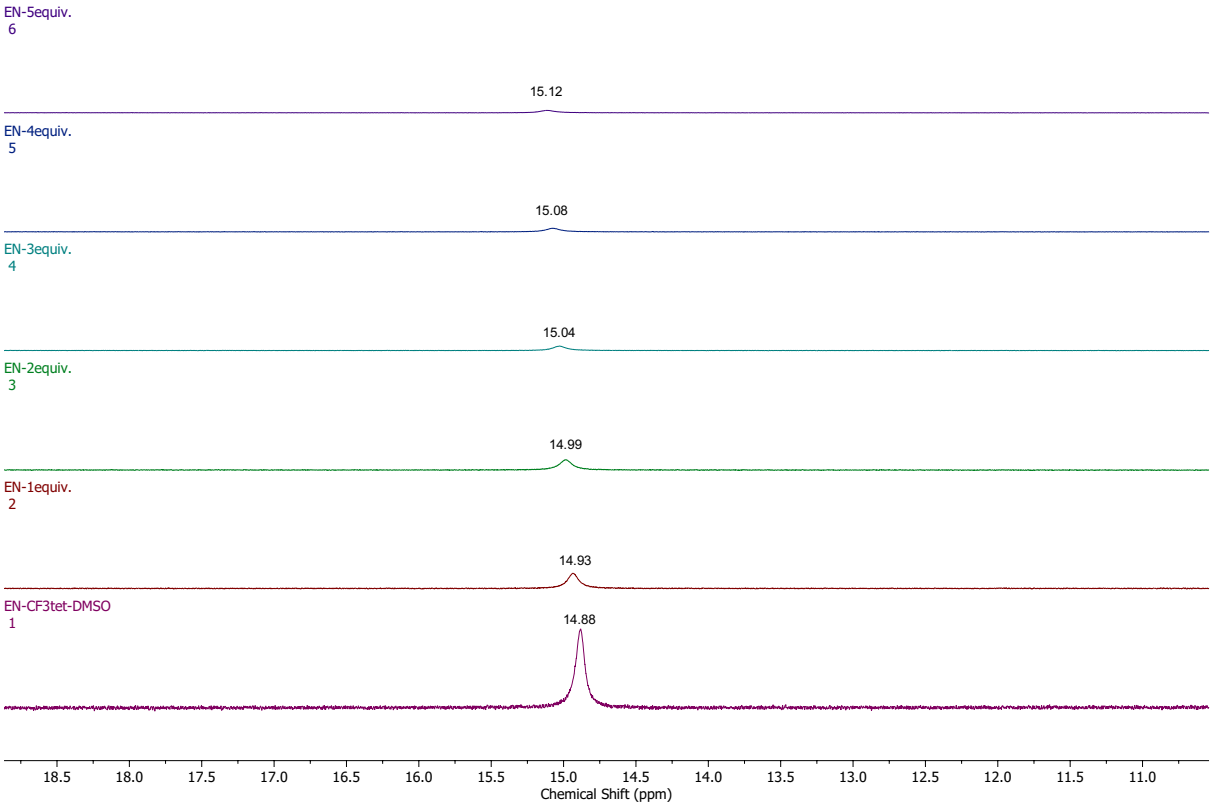

Figure S18. Partial NMR spectra showing changes in the chemical shift of NH proton during the titration of **1b** with increasing amounts of tetra butyl ammonium chloride (TBACl) in DMSO-d_6 from bottom to top.

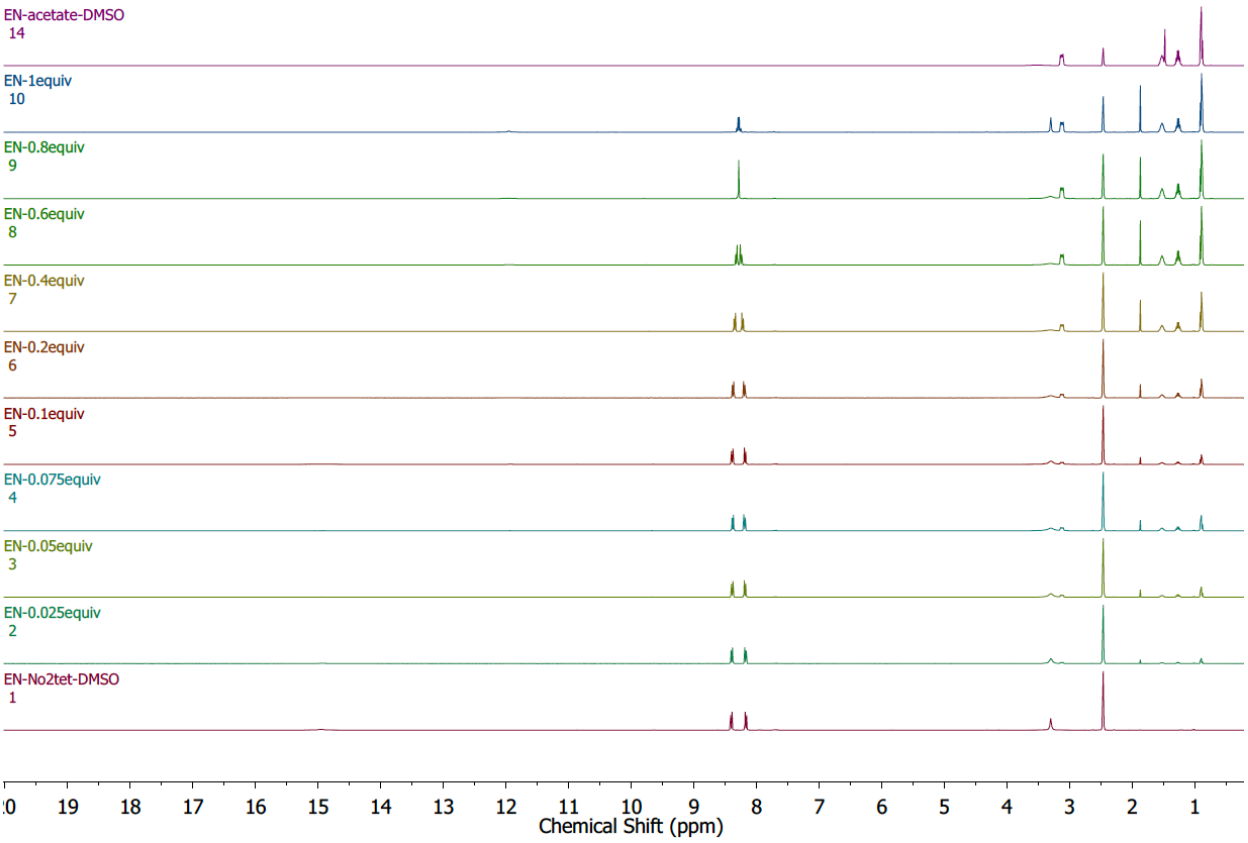

Figure S19. Full NMR spectra of **1a** in DMSO-d_6 with increasing amounts of tetra butyl ammonium acetate (TBAA) from bottom to top. The bottom spectrum is pure **1a** and the top spectrum is of pure TBAA salt in DMSO-d_6.

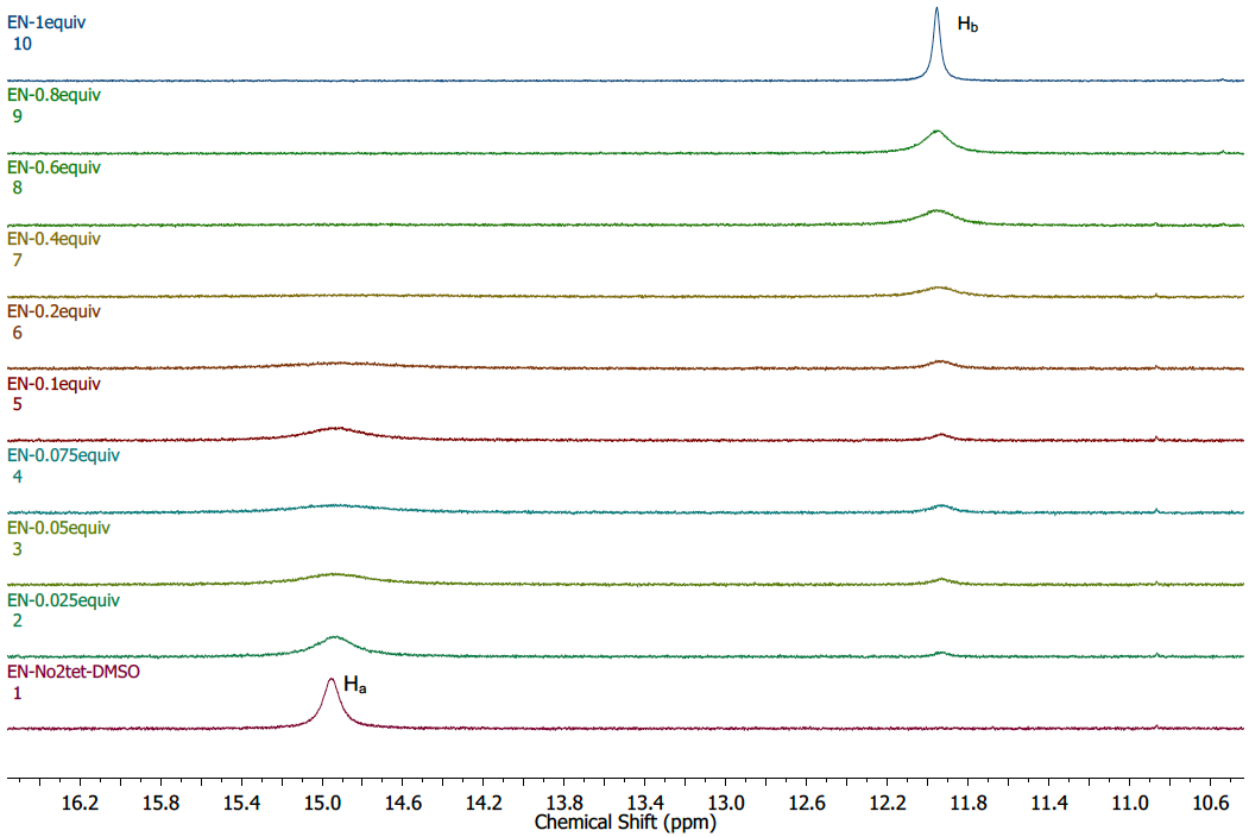

Figure S20. Partial NMR spectra during the titration of **1a** with the increasing concentration of tetra butyl ammonium acetate (TBAA) in DMSO-d_6 showing the gradual decrease in intensity of the N-H proton (H_a) and the gradual increase in the intensity of the O-H proton (H_b) indicating the formation of tetrazolonide anion **1a'** and acetic acid.

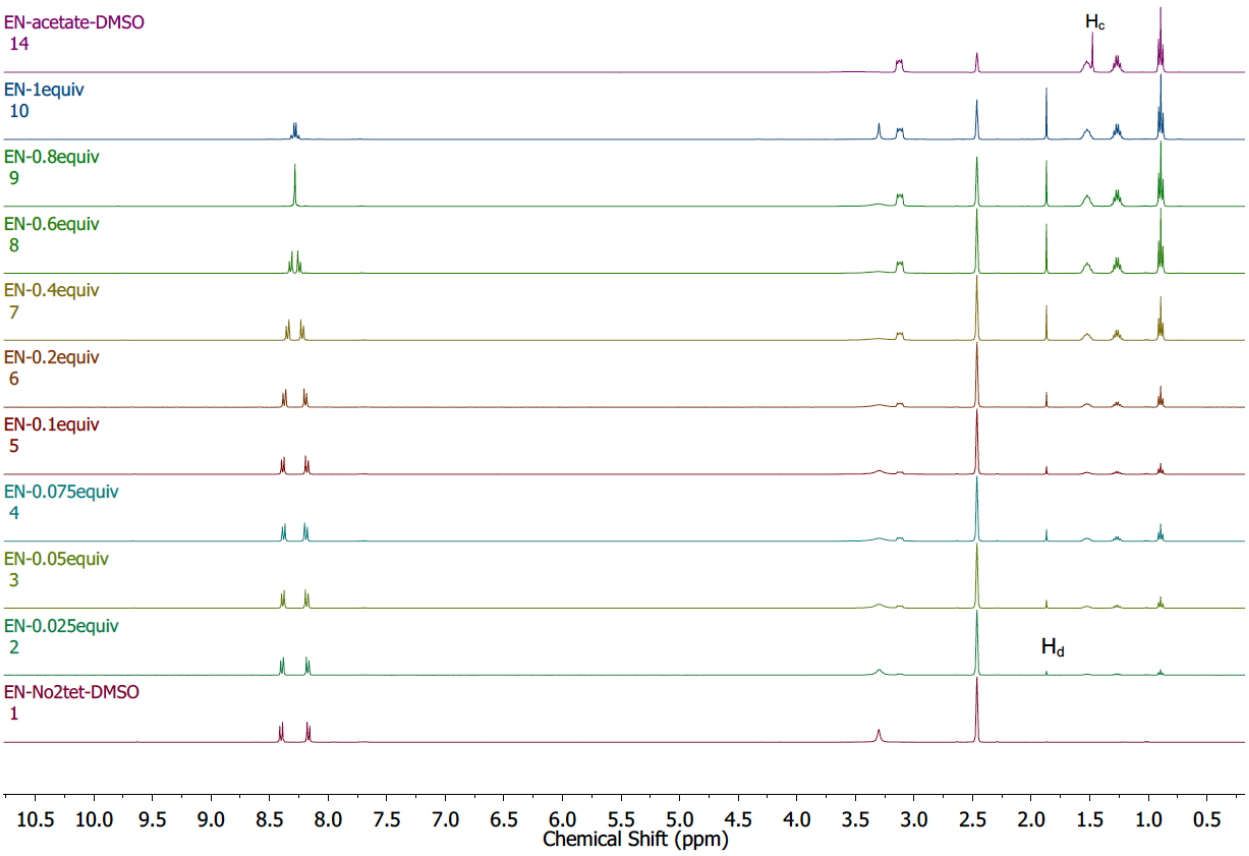

Figure S21. Partial NMR spectra during the titration of **1a** with increasing concentration of tetra butyl ammonium acetate (TBAA) in DMSO-d_6 showing aromatic peaks of **1a** as well as the acetate group peaks from TBAA and formed acetic acid ($\mathbf{H_c}$ and $\mathbf{H_d}$). The bottom spectrum is pure **1a** and the top spectrum is of pure TBAA salt in DMSO-d_6.

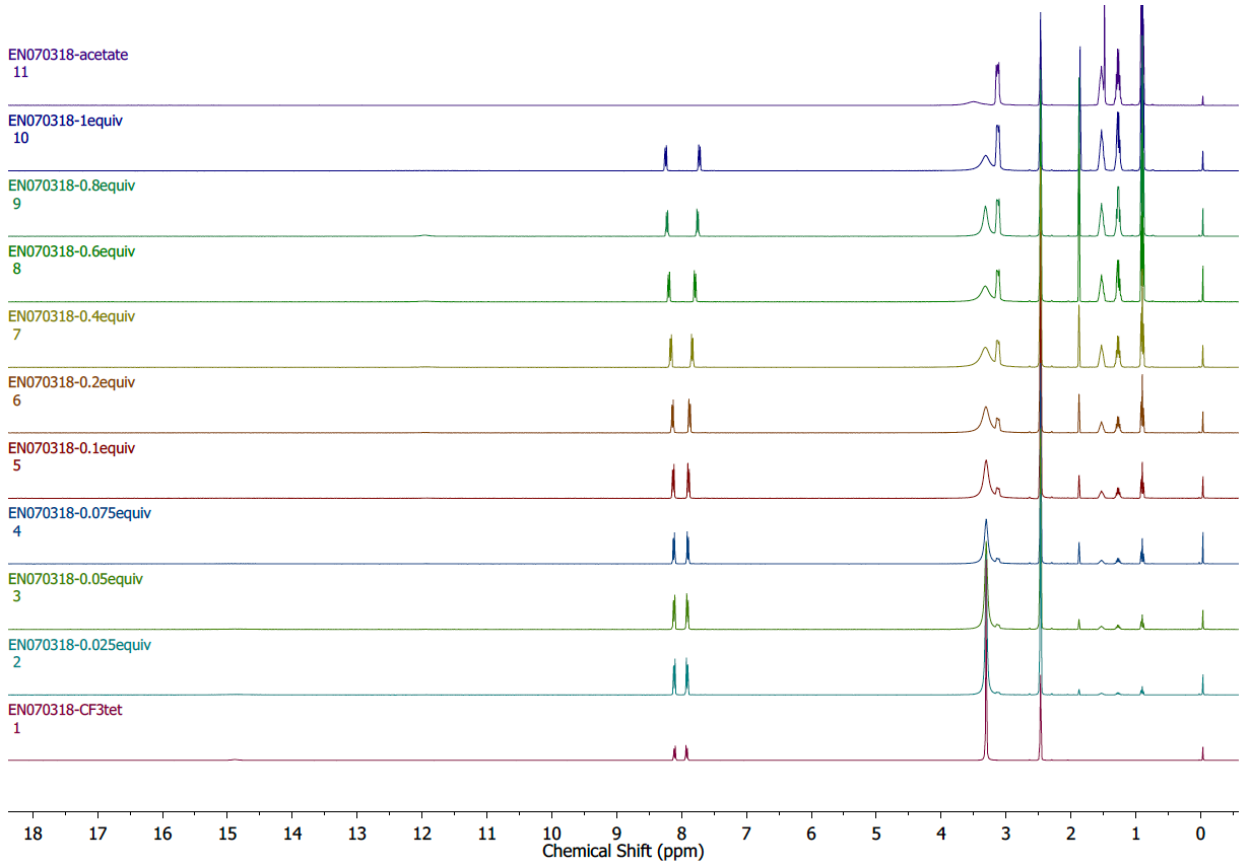

Figure S22. Full NMR spectra of **1b** in DMSO-d_6 with increasing amounts of tetra butyl ammonium acetate (TBAA) from bottom to top. The bottom spectrum is pure **1b** and the top spectrum is of pure TBAA salt in DMSO-d_6.

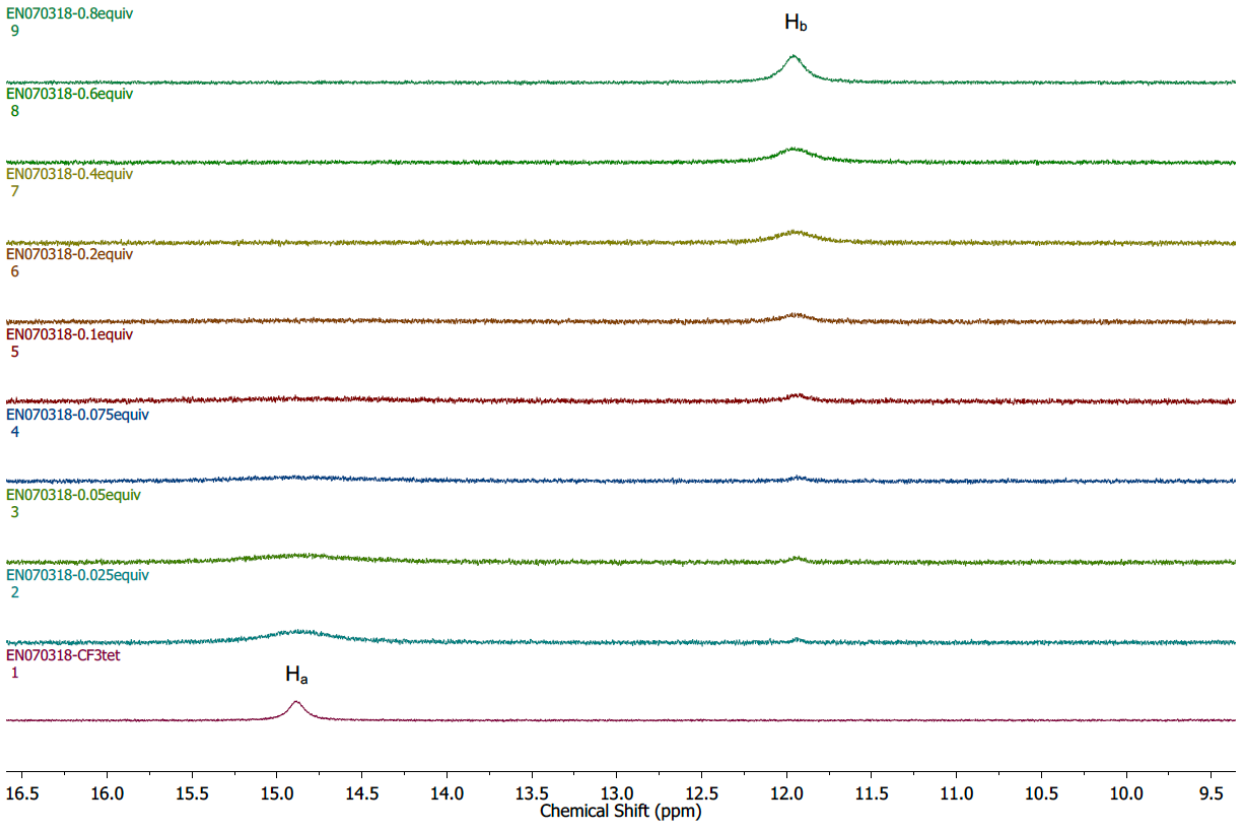

Figure S23. Partial NMR spectra during the titration of **1b** with the increasing concentration of tetra butyl ammonium acetate (TBAA) in DMSO-d_6 showing the gradual decrease in intensity of the N-H proton (H_a) and the gradual increase in the intensity of the O-H proton (H_b) indicating the formation of tetrazolonide anion **1b'** and acetic acid.

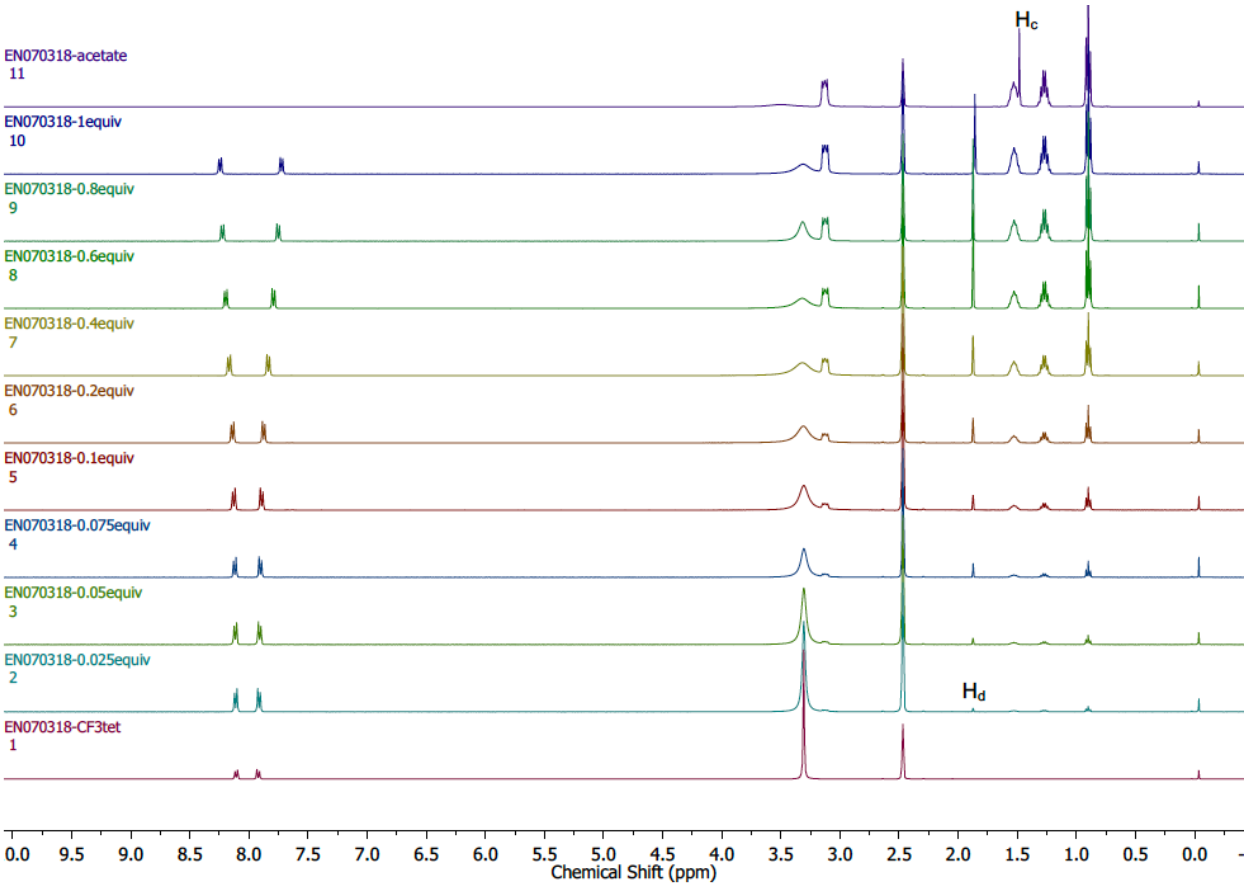

Figure S24. Partial NMR spectra during the titration of **1b** with increasing concentration of tetra butyl ammonium acetate (TBAA) in DMSO-d_6 showing aromatic peaks of 1b as well as the acetate group peaks from TBAA and formed acetic acid (H_c and H_d). The bottom spectrum is pure **1b** and the top spectrum is of pure TBAA salt in DMSO-d_6.

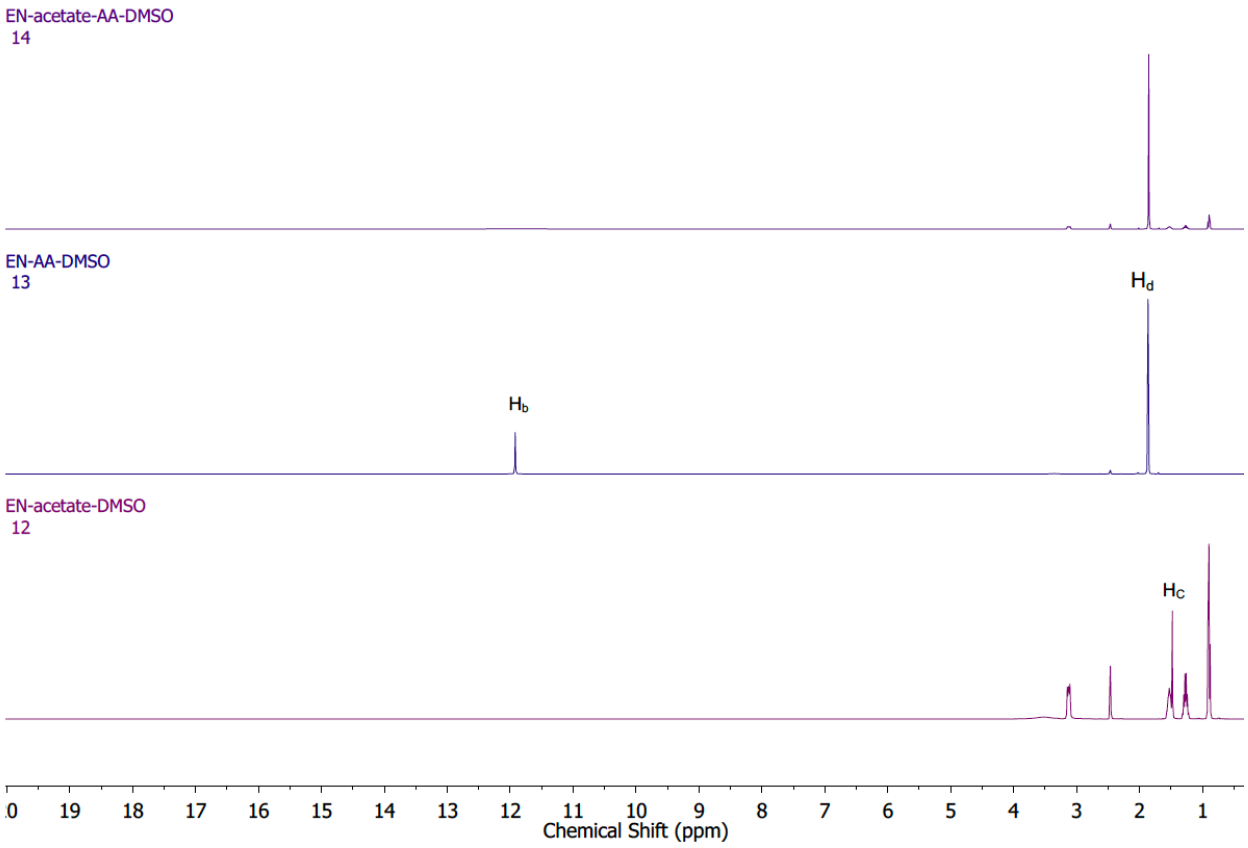

Figure S25. ^{1}H NMR spectra of tetrabutyl ammonium acetate, TBAA (bottom), acetic acid (middle), and a mixture of acetic acid and tetrabutyl ammonium acetate, TBAA (top) in DMSO-d_6. See Scheme 3 for peak labels.

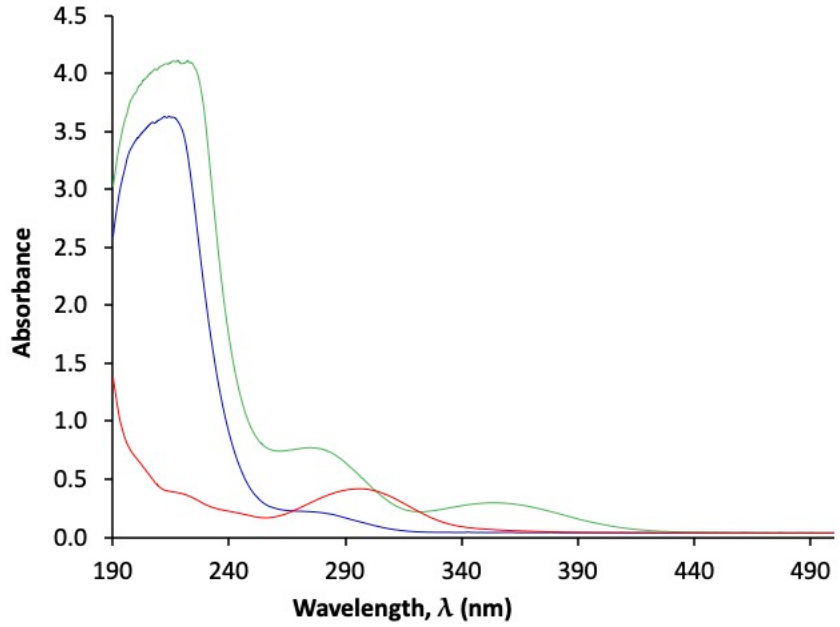

Figure S26. UV spectra showing **1a** (red); triethylamine (blue) and **1a** + 4 equivalents triethylamine (green). Upon addition of TEA to a solution of **1a** in acetonitrile, new bands emerged at 248 nm and 350 nm analogous to TBAA addition. Note that the band at 248 nm is overlapped by excess TEA.

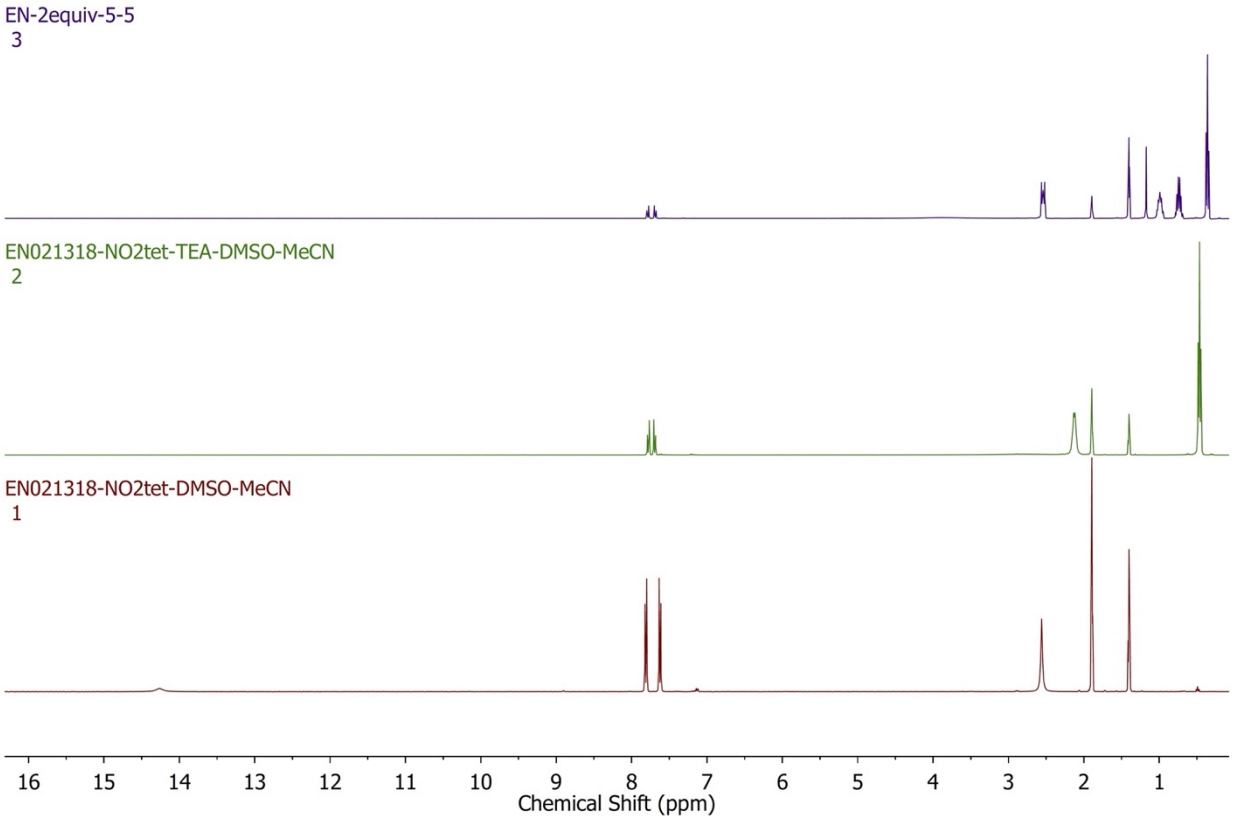

Figure S27. Full NMR spectra of **1a** in 1:1 MeCN-d_3:DMSO-d_6 (bottom), with 2 equivalents of triethylamine (center) and 2 equivalents of TBAA (top) for comparison.

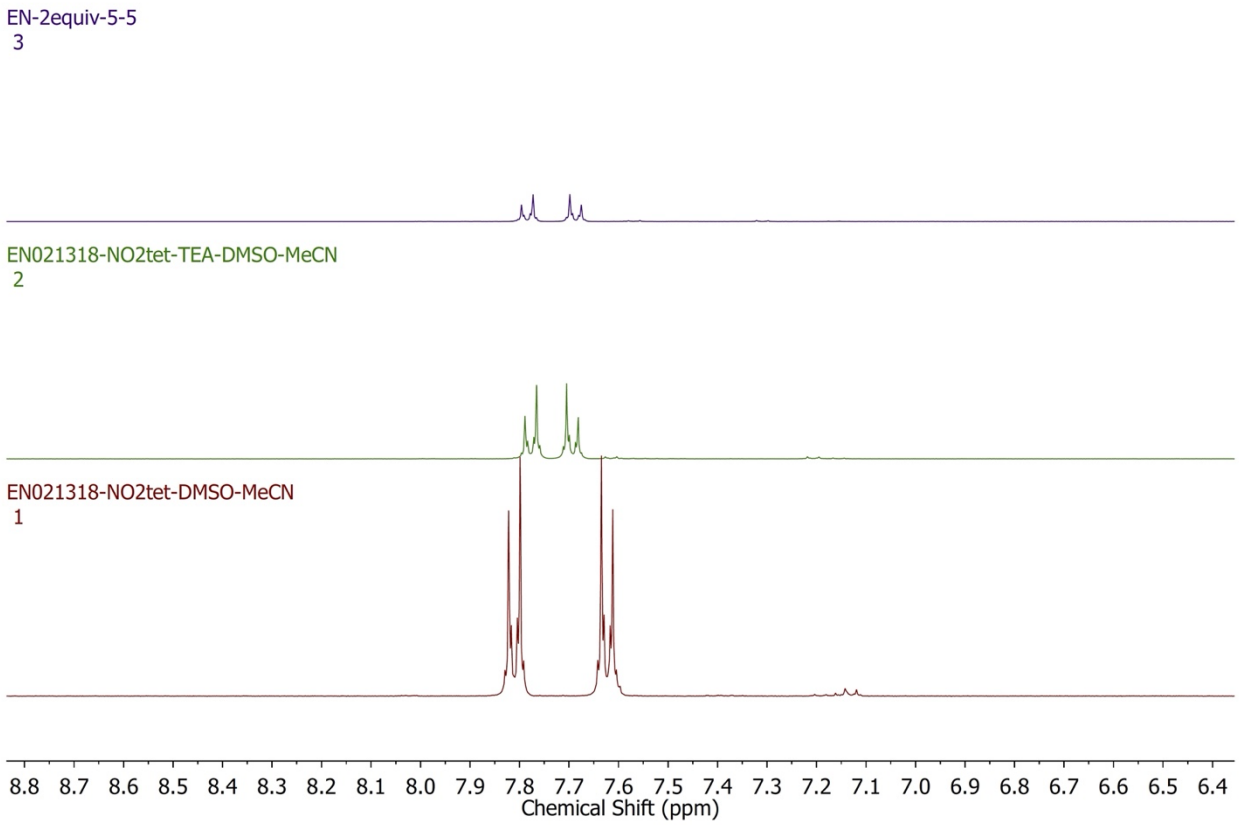

Figure S28. Partial NMR spectra of **1a** in 1:1 MeCN-d_3:DMSO-d_6 (bottom), and with 2 equivalents of triethylamine (center) as well as 2 equivalents of TBAA (top) showing the aromatic region with identical chemical shift values of the doublets.

References:

1. S. V. Rosokha, C. L. Stern, A. Swartz and R. Stewart, *Phys. Chem. Chem. Phys.*, 2014, **16**, 12968-12979.
2. M. J. Frisch, G. W. Trucks, H. B. Schlegel, G. E. Scuseria, M. A. Robb, J. R. Cheeseman, G. Scalmani, V. Barone, G. A. Petersson, H. Nakatsuji, X. Li, M. Caricato, A. Marenich, J. Bloino, B. G. Janesko, R. Gomperts, B. Mennucci, H. P. Hratchian, J. V. Ortiz, A. F. Izmaylov, J. L. Sonnenberg, D. Williams-Young, F. Ding, F. Lipparini, F. Egidi, J. Goings, B. Peng, A. Petrone, T. Henderson, D. Ranasinghe, V. G. Zakrzewski, J. Gao, N. Rega, G. Zheng, W. Liang, M. Hada, M. Ehara, K. Toyota, R. Fukuda, J. Hasegawa, M. Ishida, T. Nakajima, Y. Honda, O. Kitao, H. Nakai, T. Vreven, K. Throssell, J. Montgomery, J. A.; , J. E. Peralta, F. Ogliaro, M. Bearpark, J. J. Heyd, E. Brothers, K. N. Kudin, V. N. Staroverov, T. Keith, R. Kobayashi, J. Normand, K. Raghavachari, A. Rendell, J. C. Burant, S. S. Iyengar, J. Tomasi, M. Cossi, J. M. Millam, M. Klene, C. Adamo, R. Cammi, J. W. Ochterski, R. L. Martin, K. Morokuma, O. Farkas, J. B. Foresman and D. J. Fox, Gaussian 09, Gaussian Inc., Pittsburg, PA, 2009.
3. S. F. Boys and F. Bernardi, *Mol. Phys.*, 1970, **19**, 553-566.
4. R. Dennington, T. Keith and J. Millam, *GaussView, Version 5*, Semichem Inc., Shawnee Mission, KS, 2009.
5. S. Rayat, O. Alawode and J. Desper, *CrystEngComm*, 2009, **11**, 1892-1898.
6. T. Kitazaki, N. Tamura, A. Tasaka, Y. Matsushita, R. Hayashi, K. Okonogi and K. Itoh, *Chem. Pharm. Bull.*, 1996, **44**, 314-327.
7. P. Thordarson, *Chem. Soc. Rev.*, 2011, **40**, 1305-1323.